MAE 5730 Final Project

Robotic Surgery Dynamics Simulation

Prepared By: Sean Hughes

Sibley School of Mechanical and Aerospace Engineering
Cornell University, Ithaca, NY, USA

December 2021

I. Description

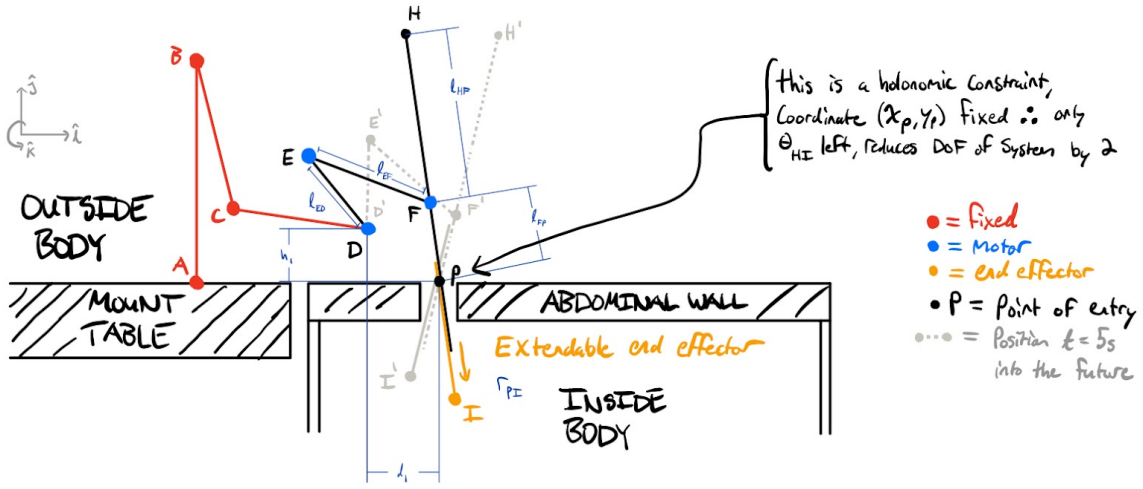

This system was developed as a model for current generation surgical robots. The dynamic system features four main linkages: the first two (DE and EF) form a standard double compound pendulum, and are meant to mount to a set of three other manually adjustable linkages—for the purpose of modeling in Matlab, these three manual linkages will be fixed. The next linkage (HP) is attached to the pendulum off-center, below its own center of gravity, and serves to model the trocar of the device. Having the attachment below its center of gravity therefore has the effect of making the linkage effectively two fixed linkages, in terms of their EOM, thus making the system 5 linkages total. Trocars are ports which are inserted into the patient's abdomen, and act as a sheath around various tools such as endoscopes and endowrists which then perform the surgery inside of the patient's abdominal cavity. It is imperative that the trochar does not inflict any undue damage to the patient's body, thus the point of insertion (point P) is modeled as a holonomic constraint which ensures that, no matter how the rest of the robot moves, that the point of entry remains in the same fixed position. Finally, the fourth linkage (PI) attaches in-line with linkage HP in order to model the sliding of the surgical tool into the abdominal cavity. This linkage therefore can slide linearly alongside linkage HP, and allows us to model the additional dynamics which the actual surgical process might incur.

Due to the precise nature of robotic surgery, this model serves as a guidepoint for developing a MIMO state-space feedback control system for which the motors at each dynamic linkage's joints could then control the motion of the device. Since this project does not involve the creation of a control system, it will be developed at a later point, working off the simulation presented in this report to do so. As such, the motion which is expected out of the robot will essentially follow that of a heavily modified

four-bar linkage (i.e. each joint follows an elliptical or circular arc), with the trochar (HP) moving the slowest (as it is directing the surgical tools), and with the other linkages moving much faster. Most importantly, all the linkages should be connected in their correct positions, and the patient point of entry should remain fixed regardless of the system's motion. This ultimately leaves 2 DOF for the robot, and forces the entire system to be determined by the 2D position of the end effector (surgical tool).

II. Analytical Model Setup

There are a number of simplifying assumptions we must make in order to model the dynamics of the robot effectively. Firstly, we will assume that the abdominal wall provides negligible normal forces on the sides of the trochar, and is of negligible thickness. We will also assume no frictional forces, as these can become quite complex to model given the inhomogeneous structure of human tissues. Additionally, we will assume that there are no reaction forces at the end effector, as we will only be modeling the motion of an endoscope, which serves as a camera and therefore does not make direct contact with the internal organs. Finally, we will assume that the end effector has negligible mass compared to the structure of the robot and trochar, which is quite reasonable considering the miniscule size of most surgical implements, especially endoscopes.

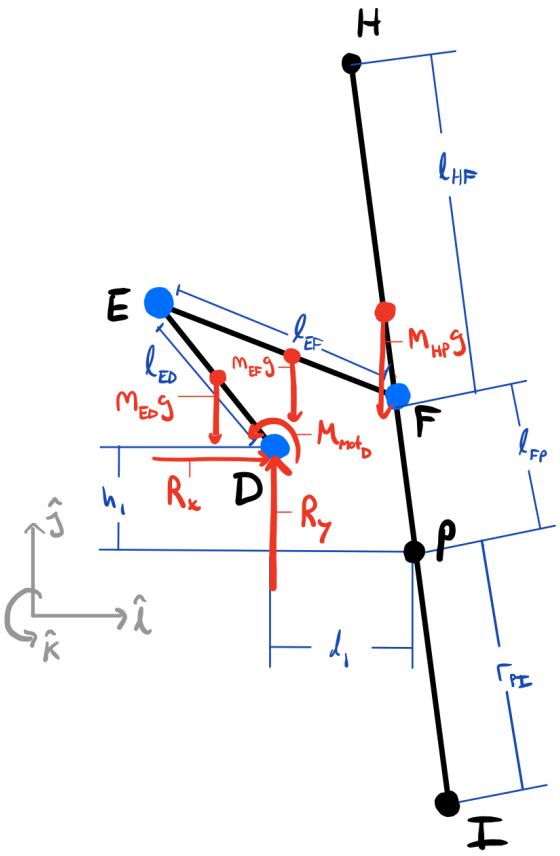

To the right is a free body diagram of the entire system; note that, because of our underlying assumptions, the robot effectively moves in free space. This is an important feature of every surgical robot, as they are optimized to inflict as little damage to the patient as possible, and are therefore isolated from all other forces besides the force that it applies to the internal tissues during surgery. This point, in particular, is why such high precision and resolution is required for these devices, as the entirety of the system's dynamics moves downstream all to affect only one point at the end effector, which makes direct contact with the internal organs. Finally, note that each blue point represents a motorized joint for the system; we will be modeling our

EOM later with these motors taken into account, however they will be turned off for the animation since no control system was developed thus far.

There are 12 DOF in total before applying constraints, 3 for each linkage. 2 DOF are removed for each point, D, E, F, and P, due to the constraint that each linkage's length remains constant and attached to the linkage prior. The last 2 DOF are removed via the holonomic constraint applied at the point of insertion, P, which fixes its location with respect to the origin, D, therefore giving 12 - (2*(4) + 2) = 2 DOF for the system. If a control system were to be implemented, then the 3 motors would account for 3 rheonomic, non-holonomic constraints on the angular velocity of each linkage.

Finally, note that we will be tracking several groups of coordinates due to the complex nature of this system. First, we will be tracking the x and y positions and velocities of three centers of mass, one at each of the red dots in the FBD. We will then track the x and y positions and velocities of each joint, as well as important points along the trocar: E, F, H, P. In addition, we will track the radial position and radial velocity of the end effector, PI. Finally, we will be tracking the angles and angular velocities of linkages DE, EF, and HP, with each angle measured counterclockwise from the +jhat direction in every case.

III. Equations of Motion (DAE Approach)

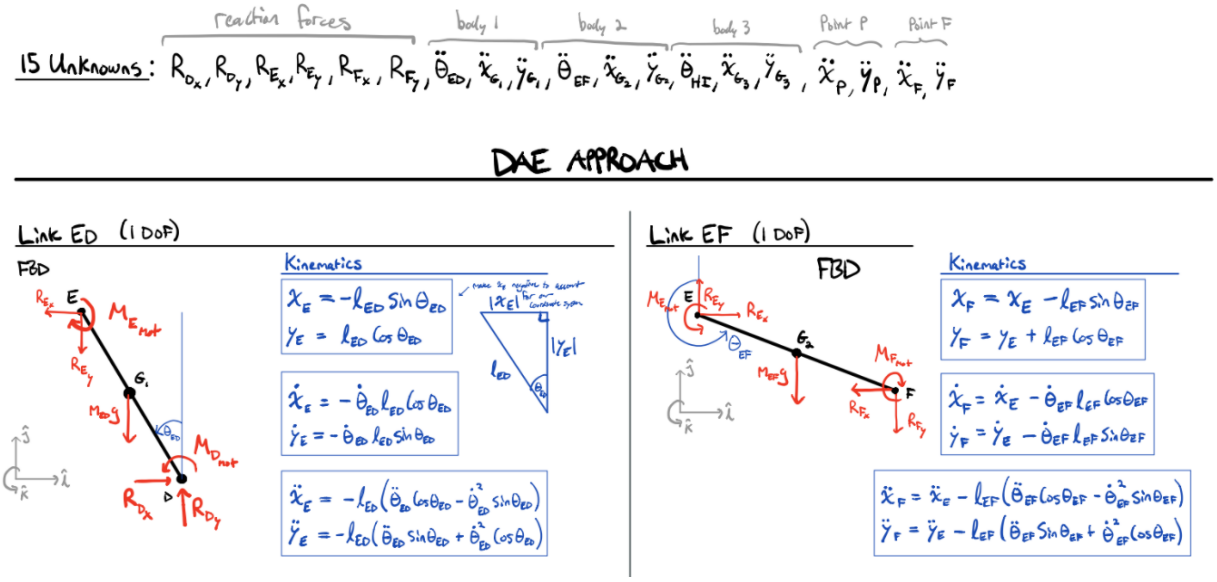

For x_{G_1}/y_{G_1} and associated derivatives, only replace l_{ED} with $l_{ED}/2$ for boxed eqs above

$$\vec{r}_{D/G_1} = -\frac{x_E}{2}\hat{\imath} - \frac{y_E}{2}\hat{\jmath} \qquad \vec{r}_{E/G_1} = \frac{x_E}{2}\hat{\imath} + \frac{y_E}{2}\hat{\jmath}$$

Kinetics

ΔMB about Point G_1:

$$\sum \vec{M}_{G_1} = \dot{\vec{H}}_{tot/G_1}$$

$$\vec{M}_{D_{tot}} - \vec{M}_{E_{tot}} + \vec{r}_{D/G_1} \times (R_{D_x}\hat{\imath} + R_{D_y}\hat{\jmath}) + \vec{r}_{E/G_1} \times (-R_{E_x}\hat{\imath} - R_{E_y}\hat{\jmath}) = \ddot{\theta}_{ED} I_{ED} \hat{k}$$

$$= \left(-\frac{x_E}{2}\hat{\imath} - \frac{y_E}{2}\hat{\jmath}\right) \times (R_{D_x}\hat{\imath} + R_{D_y}\hat{\jmath}) \qquad = \left(\frac{x_E}{2}\hat{\imath} + \frac{y_E}{2}\hat{\jmath}\right) \times (-R_{E_x}\hat{\imath} - R_{E_y}\hat{\jmath})$$

$$= -\frac{x_E}{2}R_{D_y} + \frac{y_E}{2}R_{D_x} \qquad = -\frac{x_E}{2}R_{E_y} + \frac{y_E}{2}R_{E_x}$$

$$\boxed{M_{D_{tot}} - M_{E_{tot}} - \frac{x_E}{2}R_{D_y} + \frac{y_E}{2}R_{D_x} - \frac{x_E}{2}R_{E_y} + \frac{y_E}{2}R_{E_x} = \ddot{\theta}_{ED} I_{ED}} \quad (1)$$

LMB in $\hat{\imath}$-direction

$$\sum \vec{F}\cdot\hat{\imath} = M_{ED}\ddot{x}_{G_1}$$

$$\boxed{R_{D_x} - R_{E_x} = M_{ED}\ddot{x}_{G_1}} \quad (2)$$

LMB in $\hat{\jmath}$-direction

$$\sum \vec{F}\cdot\hat{\jmath} = M_{ED}\ddot{y}_{G_1}$$

$$\boxed{R_{D_y} - R_{E_y} - M_{ED}g = M_{ED}\ddot{y}_{G_1}} \quad (3)$$

For x_{G_2}/y_{G_2} and associated derivatives, only replace l_{EF} with $l_{EF}/2$ for boxed eqs above,

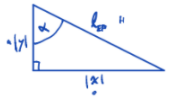

$$\sin(\theta_1 - \theta_2) = \sin(\theta_1)\cos(\theta_2) - \cos(\theta_1)\sin(\theta_2)$$
$$\sin(\theta_1 - 180^\circ) = \sin\theta_1\cos(180^\circ) - \cos\theta_1\sin(180^\circ) = -\sin\theta_1$$
$$\cos(\theta_1 - \theta_2) = \cos(\theta_1)\cos(\theta_2) + \sin(\theta_1)\sin(\theta_2)$$
$$\cos(\theta_1 - 180^\circ) = \cos\theta_1(\cos(180^\circ) + \sin(\theta_1)\sin(180^\circ) = -\cos\theta_1$$

$$\alpha = \theta_{EP} - 180^\circ$$
$$|x| = l_{EP}\sin\alpha = l_{EP}\sin(\theta_{EP} - 180) = -l_{EP}\sin\theta_{EP}$$
$$|y| = l_{EP}\cos\alpha = l_{EP}\cos(\theta_{EP} - 180) = -l_{EP}\cos\theta_{EP}$$

make negative to account for our coordinate system $\therefore$ plug $l_{EP}\cos\theta_{EP}$

$$\vec{r}_{F/G_2} = \frac{-l_{EP}}{2}\sin\theta_{EP}\,\hat{\imath} + \frac{l_{EP}}{2}\cos\theta_{EP}\,\hat{\jmath}$$
$$\vec{r}_{E/G_2} = \frac{l_{EP}}{2}\sin\theta_{EP}\,\hat{\imath} - \frac{l_{EP}}{2}\cos\theta_{EP}\,\hat{\jmath}$$

Kinetics

LMB in $\hat{\imath}$-direction

$$\sum \vec{F}\cdot\hat{\imath} = M_{EF}\ddot{x}_{G_2}$$

$$\boxed{R_{E_x} - R_{F_x} = M_{EF}\ddot{x}_{G_2}} \quad (4)$$

LMB in $\hat{\jmath}$-direction

$$\sum \vec{F}\cdot\hat{\jmath} = M_{EF}\ddot{y}_{G_2}$$

$$\boxed{R_{E_y} - R_{F_y} - M_{EF}g = M_{EF}\ddot{y}_{G_2}} \quad (5)$$

ΔMB about Point G_2:

$$\sum \vec{M}_{G_2} = \dot{\vec{H}}_{tot/G_2}$$

$$\vec{M}_{E_{tot}} - \vec{M}_{F_{tot}} + \vec{r}_{F/G_2} \times (-R_{F_x}\hat{\imath} - R_{F_y}\hat{\jmath}) + \vec{r}_{E/G_2} \times (R_{E_x}\hat{\imath} + R_{E_y}\hat{\jmath}) = \ddot{\theta}_{EF} I_{EF} \hat{k}$$

$$\vec{M}_{E_{tot}} - \vec{M}_{F_{tot}} + \left(\frac{-l_{EP}}{2}\sin\theta_{EP}\,\hat{\imath} + \frac{l_{EP}}{2}\cos\theta_{EP}\,\hat{\jmath}\right) \times (-R_{F_x}\hat{\imath} - R_{F_y}\hat{\jmath}) + \left(\frac{l_{EP}}{2}\sin\theta_{EP}\,\hat{\imath} - \frac{l_{EP}}{2}\cos\theta_{EP}\,\hat{\jmath}\right) \times (R_{E_x}\hat{\imath} + R_{E_y}\hat{\jmath}) = \ddot{\theta}_{EF} I_{EF} \hat{k}$$

$$\boxed{M_{E_{tot}} - M_{F_{tot}} + \frac{l_{EP}}{2}R_{F_y}\sin\theta_{EP} + \frac{l_{EP}}{2}R_{F_x}\cos\theta_{EP} + \frac{l_{EP}}{2}R_{E_y}\sin\theta_{EP} + \frac{l_{EP}}{2}R_{E_x}\cos\theta_{EP} = \ddot{\theta}_{EF} I_{EF}} \quad (6)$$

Link HP + PI (1 DOF + 1 DOF)

FBD

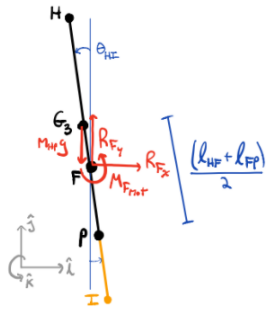

Kinematics

$$x_P = x_F + l_{FP}\sin\theta_{HI} \qquad y_P = y_F - l_{FP}\cos\theta_{HI}$$

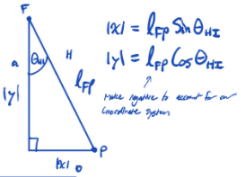

$$|x| = l_{FP}\sin\theta_{HI} \qquad |y| = l_{FP}\cos\theta_{HI}$$

make negative to account for our coordinate system

$$x_I = x_P + r_{PI}\sin\theta_{HI} \qquad y_I = y_P - r_{PI}\cos\theta_{HI}$$

$$\dot{x}_P = \dot{x}_F + \dot{\theta}_{HI} l_{FP}\cos\theta_{HI} \qquad \dot{y}_P = \dot{y}_F + \dot{\theta}_{HI} l_{FP}\sin\theta_{HI}$$

$$\dot{x}_I = \dot{x}_P + \dot{r}_{PI}\sin\theta_{HI} + r_{PI}\dot{\theta}_{HI}\cos\theta_{HI} \qquad \dot{y}_I = \dot{y}_P - \dot{r}_{PI}\cos\theta_{HI} + r_{PI}\dot{\theta}_{HI}\sin\theta_{HI}$$

$$\ddot{x}_P = \ddot{x}_F + l_{FP}\left(\ddot{\theta}_{HI}\cos\theta_{HI} - \dot{\theta}_{HI}^2\sin\theta_{HI}\right) \qquad \ddot{y}_P = \ddot{y}_F + l_{FP}\left(\ddot{\theta}_{HI}\sin\theta_{HI} + \dot{\theta}_{HI}^2\cos\theta_{HI}\right)$$

$$\ddot{x}_I = \ddot{x}_P + \left(\dot{r}_{PI}\sin\theta_{HI} + \dot{r}_{PI}\dot{\theta}_{HI}\cos\theta_{HI}\right) + \left[\dot{r}_{PI}\left(\dot{\theta}_{HI}\cos\theta_{HI}\right) + r_{PI}\left(\ddot{\theta}_{HI}\cos\theta_{HI} - \dot{\theta}_{HI}^2\sin\theta_{HI}\right)\right]$$

$$\ddot{y}_I = \ddot{y}_P - \left(\dot{r}_{PI}\cos\theta_{HI} - \dot{r}_{PI}\dot{\theta}_{HI}\sin\theta_{HI}\right) + \left[\dot{r}_{PI}\left(\dot{\theta}_{HI}\sin\theta_{HI}\right) + r_{PI}\left(\ddot{\theta}_{HI}\sin\theta_{HI} + \dot{\theta}_{HI}^2\cos\theta_{HI}\right)\right]$$

$$\ddot{x}_I = \ddot{x}_P + \dot{r}_{PI}\sin\theta_{HI} + 2\dot{r}_{PI}\dot{\theta}_{HI}\cos\theta_{HI} + r_{PI}\left(\ddot{\theta}_{HI}\cos\theta_{HI} - \dot{\theta}_{HI}^2\sin\theta_{HI}\right)$$

$$\ddot{y}_I = \ddot{y}_P - \dot{r}_{PI}\cos\theta_{HI} + 2\dot{r}_{PI}\dot{\theta}_{HI}\sin\theta_{HI} + r_{PI}\left(\ddot{\theta}_{HI}\sin\theta_{HI} + \dot{\theta}_{HI}^2\cos\theta_{HI}\right)$$

$$l_{G_3F} = \frac{(l_{HP}+l_{FP})}{2} - l_{FP} = \frac{(l_{HP}-l_{FP})}{2}$$

$$\vec{r}_{F/G_3} = -\vec{r}_{G_3/F}$$ ↓ in $-x$ direction, in $+y$ direction

$$= -\left[-\frac{(l_{HP}-l_{FP})}{2}\sin\theta_{HI}\,\hat{\imath} + \frac{(l_{HP}-l_{FP})}{2}\cos\theta_{HI}\,\hat{\jmath}\right]$$

$$\boxed{\vec{r}_{F/G_3} = \frac{(l_{HP}-l_{FP})}{2}\sin\theta_{HI}\,\hat{\imath} - \frac{(l_{HP}-l_{FP})}{2}\cos\theta_{HI}\,\hat{\jmath}}$$

Kinetics

LMB in $\hat{\imath}$-direction

$$\sum \vec{F}\cdot\hat{\imath} = M_{HP}\,\ddot{x}_{G_3}$$

$$\boxed{R_{F_x} = M_{HP}\,\ddot{x}_{G_3}} \quad (7)$$

LMB in $\hat{\jmath}$-direction

$$\sum \vec{F}\cdot\hat{\jmath} = M_{HP}\,\ddot{y}_{G_3}$$

$$\boxed{R_{F_y} - M_{HP}g = M_{HP}\,\ddot{y}_{G_3}} \quad (8)$$

AMB about Point G_3:

$$\sum \vec{M}_{G_3} = \dot{\vec{H}}_{tot/G_3}$$

$$\vec{M}_{F_{mot}} + \vec{r}_{F/G_3}\times\left(R_{F_x}\hat{\imath} + R_{F_y}\hat{\jmath}\right) = \ddot{\theta}_{EF} I_{EF}\hat{k}$$

$$\vec{M}_{F_{mot}} + \left[\frac{(l_{HP}-l_{FP})}{2}\sin\theta_{HI}\,\hat{\imath} - \frac{(l_{HP}-l_{FP})}{2}\cos\theta_{HI}\,\hat{\jmath}\right]\times\left(R_{F_x}\hat{\imath} + R_{F_y}\hat{\jmath}\right) = \ddot{\theta}_{HI} I_{HP}\hat{k}$$

$$\boxed{M_{F_{mot}} + \frac{(l_{HP}-l_{FP})}{2}R_{F_y}\sin\theta_{HI} + \frac{(l_{HP}-l_{FP})}{2}R_{F_x}\cos\theta_{HI} = \ddot{\theta}_{HI} I_{HP}} \quad (9)$$

Holonomic Constraint

$x_P = d_1$	$\dot{x}_P = 0$	$\ddot{x}_P = 0$
$y_P = -h_1$	$\dot{y}_P = 0$	$\ddot{y}_P = 0$

A

	R_{D_x}	R_{D_y}	R_{E_x}	R_{E_y}	R_{F_x}	R_{F_y}	$\ddot{\theta}_{ED}$	$\ddot{x}_{G_1}$	$\ddot{y}_{G_1}$	$\ddot{\theta}_{EF}$	$\ddot{x}_{G_2}$	$\ddot{y}_{G_2}$	$\ddot{\theta}_{HI}$	$\ddot{x}_{G_3}$	$\ddot{y}_{G_3}$	$\ddot{x}_P$	$\ddot{y}_P$	$\ddot{x}_F$	$\ddot{y}_F$
1	$\frac{y_E}{2}$	$-\frac{x_E}{2}$	$\frac{y_E}{2}$	$-\frac{x_E}{2}$	0	0	$-I_{ED}$	0	0	0	0	0	0	0	0				
2	1	0	-1	0	0	0	0	$-M_{ED}$	0	0	0	0	0	0	0				
3	0	1	0	-1	0	0	0	0	$-M_{ED}$	0	0	0	0	0	0				
4	0	0	1	0	-1	0	0	0	0	0	$-M_{EF}$	0	0	0	0				
5	0	0	0	1	0	-1	0	0	0	0	0	$-M_{EF}$	0	0	0				
6	0	0	C	S	C	S	0	0	0	$-I_{EF}$	0	0	0	0	0				
7	0	0	0	0	1	0	0	0	0	0	0	0	0	$-M_{HP}$	0				
8	0	0	0	0	0	1	0	0	0	0	0	0	0	0	$-M_{HP}$				
9	0	0	0	0	C2	S2	0	0	0	0	0	0	$-I_{HE}$	0	0				
10	0	0	0	0	0	0	$\frac{l_{ED}}{2}\cos\theta_{ED}$	1	0	0	0	0	0	0	0				
11	0	0	0	0	0	0	$\frac{l_{ED}}{2}\sin\theta_{ED}$	0	1	0	0	0	0	0	0				
12	0	0	0	0	0	0	0	-2	0	$\frac{l_{EF}}{2}\cos\theta_{EF}$	1	0	0	0	0				
13	0	0	0	0	0	0	0	0	-2	$\frac{l_{EF}}{2}\sin\theta_{EF}$	0	1	0	0	0				
14								0	$l_{G_3P}\cos\theta_{HI}$	1	0	0	0	-1	0				
15								0	$l_{G_3F}\sin\theta_{HI}$	0	1	0	0	0	-1				
16										1	0	0	0						
17										0	1	0	0						
18								0	$-l_{HP}\cos\theta_{HI}$	0	0	1	0	-1	0				
19								0	$-l_{HP}\sin\theta_{HI}$	0	0	0	1	0	-1				

$$=$$

B

1	$M_{E_{mot}} - M_{D_{mot}}$
2	0
3	$M_{ED}g$
4	0
5	$M_{EF}g$
6	$M_{F_{mot}} - M_{E_{mot}}$
7	0
8	$M_{HP}g$
9	$-M_{F_{mot}}$
10	$\frac{l_{ED}}{2}\dot{\theta}_{ED}^2\sin\theta_{ED}$
11	$-\frac{l_{ED}}{2}\dot{\theta}_{ED}^2\cos\theta_{ED}$
12	$\frac{l_{EF}}{2}\dot{\theta}_{EF}^2\sin\theta_{EF}$
13	$-\frac{l_{EF}}{2}\dot{\theta}_{EF}^2\cos\theta_{EF}$
14	$l_{G_3F}\dot{\theta}_{HI}^2\sin\theta_{HI}$
15	$-l_{G_3F}\dot{\theta}_{HI}^2\cos\theta_{HI}$
16	0
17	0
18	$-l_{FP}\dot{\theta}_{HI}^2\sin\theta_{HI}$
19	$l_{FP}\dot{\theta}_{HI}^2\cos\theta_{HI}$

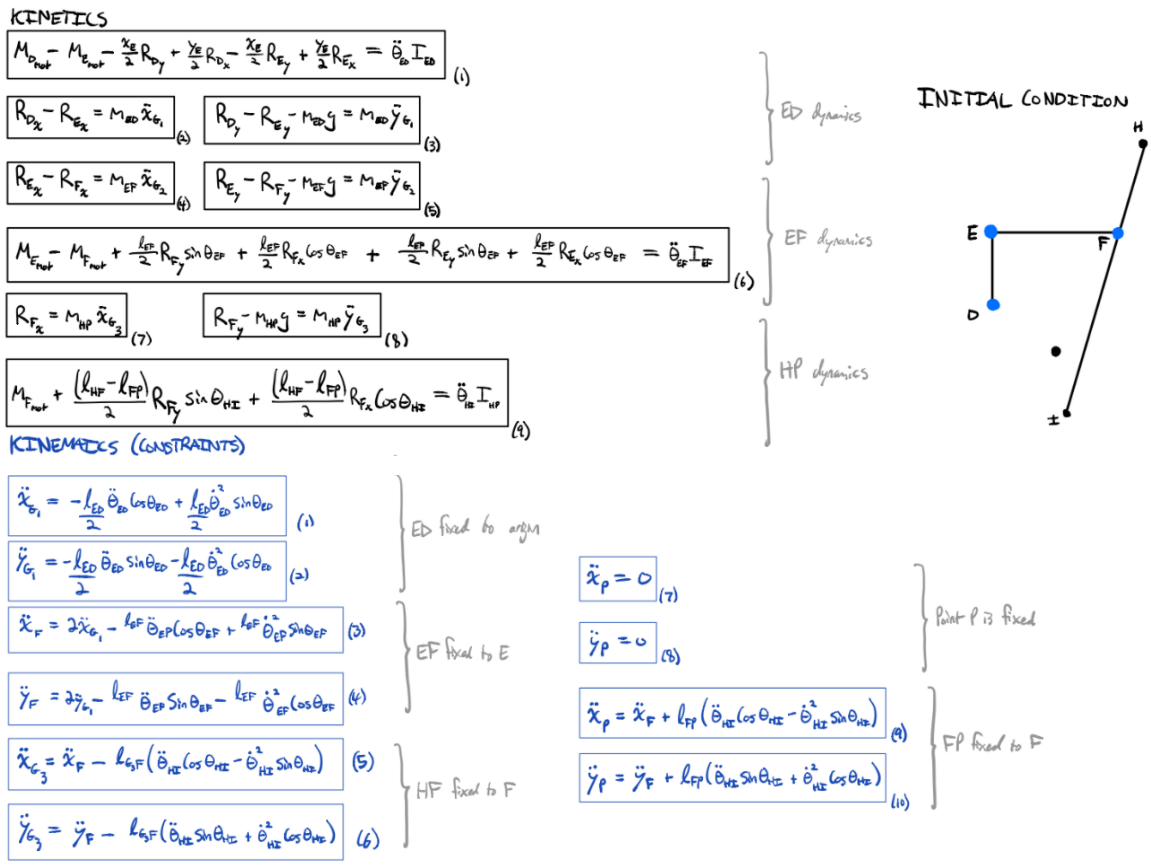

Note that, here we see how our 12 DOF gets reduced by 10 constraint equations into 2 DOF total. The description of what each equation does can be found in gray, bracketed to the right. In addition, the initial condition for this system includes 19 variables, which necessitated the creation of an additional function, *kinematic_processing_ICs.m*; this function uses many of the same kinematic equations derived above, except in a different order, and only focusing on the joint positions in particular. This function takes in a 4 variable state (2 DOF for position and velocity) which specifies the angle of linkage ED, the position of the end effector, and their respective velocities. It also takes in the other two linkage angles, and determines the position for the point of entry, point P, using these extra angles. Within the function is a description of why this process must be done, but it effectively allows for the system to remain solvable without needing to use nonlinear dynamics techniques.

The equations developed for the DAE approach above are just slight modifications of the kinematic equations developed from the free body diagrams, in that they use the length of the point of interest to the center of gravity, rather than the length of the entire linkage. However, this C.O.G. length is always a simple fraction of the linkage length, thus making it easily resolvable from the preexisting derivations.

IV. Animation

Initial State:

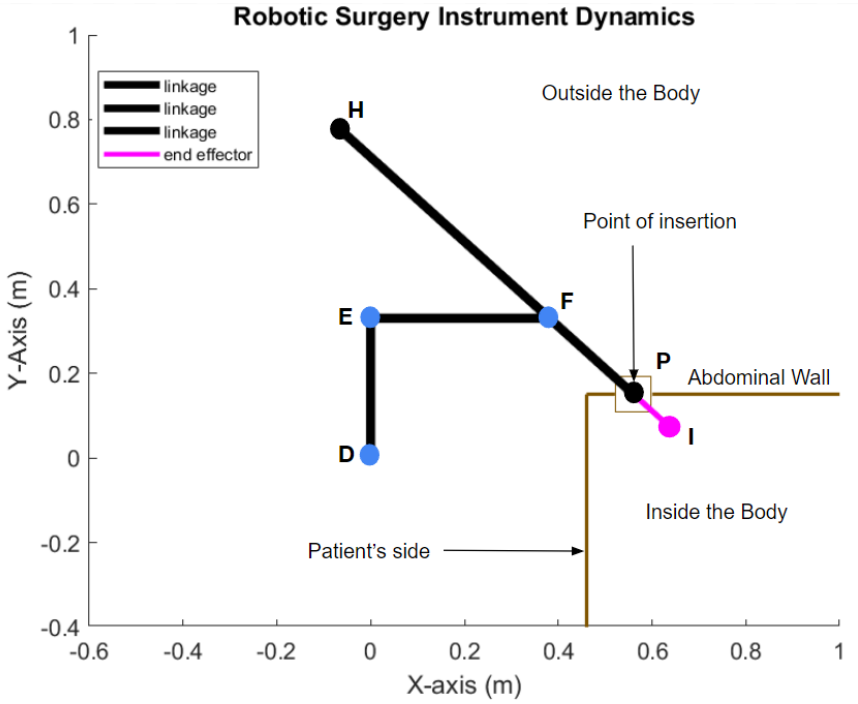

Final State:

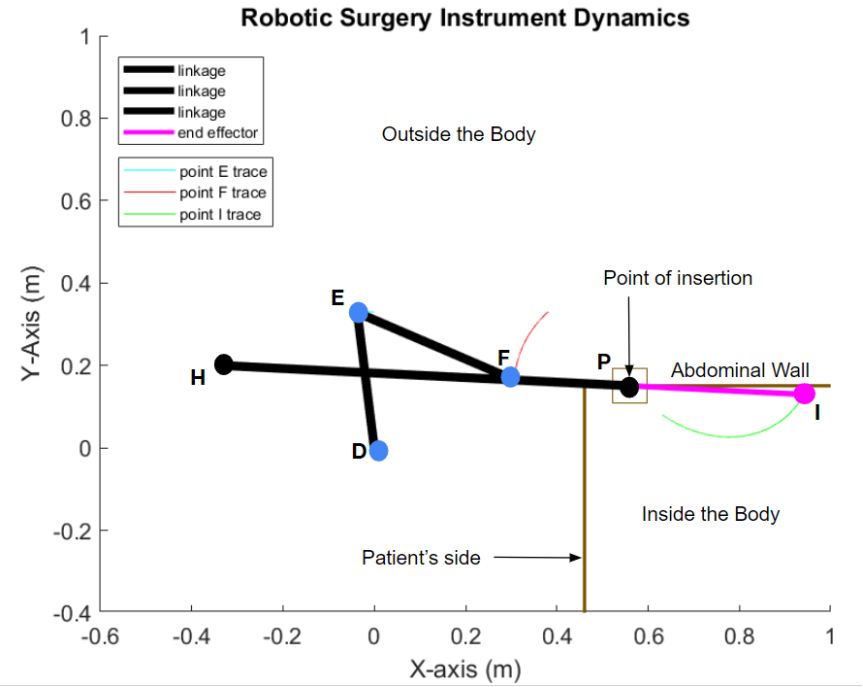

As can be seen from the still frames from the animation above, the device follows the expected motion laid out earlier, having each joint follow an elliptical arc as a result of the 1 DOF afforded to the angle, and the 1 DOF afforded to the linear

actuation of the end effector. The point of insertion remains constant throughout the entire animation, thus demonstrating the successful integration of constraints throughout the entire dynamic system.

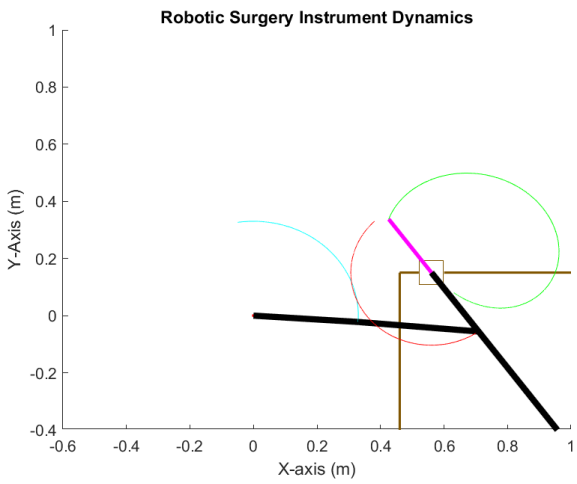

An approximation of the patient's body has been plotted as well, corresponding to the brown lines in each still frame. The end effector displays a possible range of motion which is consistent with surgical applications; the end effector actuates linearly in-and-out (for this animation it is given a sinusoidal control input) and interacts with the organs along the patient's abdominal wall, as would be required for an endoscope during a hysterectomy (a common robotic surgery). Despite this, there is no control system to direct the device. Thus, as can be seen in the above plot at a later time, the robot does in-fact display motion which would be inconsistent with surgery due to it ignoring the abdominal wall boundary. However, as we have discussed earlier, this project is purely a demonstration of the fundamental dynamics of the system, such that a control system could be developed using this simulation, at a later date. The animation therefore provides a clear framework for which to base a control system off of, and demonstrates realistic dynamics in-line with what we expect from our equations of motion.

VI. Discussion

In order to confirm the validity of our results, below are the error plots for the length of each linkage and the position for the point of entry corresponding to the constraints we set out earlier. As we can see, in every case, the error is <1e-12, which was what we set out in the options for our numerical integrator. This therefore provides us with the confidence that these results are accurate.

Furthermore, because we have set up our equations of motion using the motor torques as a variable, we can now use this simulation in order to test different motor stall torques and determine which provides an adequate amount of resistance to rotation, as well as an adequate additional torque for the future control system. This can be seen within the dynamics function *RSI_Dynamics_DAE.m*.

One problem encountered by the animation which was unforeseen was that the end effector linkage actually moves more dramatically at the beginning, with the linkage ED barely moving at all. This is in direct contrast with what we originally expected for

the system's dynamics; however, about halfway through the animation, the velocity of the two linkages switches and linkage ED starts moving much more dramatically, while the end effector moves very slowly. This therefore points us towards an important characteristic of the robot, in that, due to the chaotic motion involved with triple pendulums, the relative motion of each link cannot be simply related. This therefore means that our future control system will have to control not just the angle and position of the end effector (2 DOF), but also the angles of each linkage, such that they do not accelerate extremely fast as a result of small disturbances at the end effector. If this were not accounted for, then the robot could move erratically and be a danger to the surgeons and nurses using it.

Ultimately, the system has dynamics that are both confirmed to be accurate, as well as follow our intuitive expectation for its motion. This simulation provides a good basis for which a feedback control system could be developed in the future, and as such, provides valuable information for its design without the need of expensive biomedical equipment or prototyping. The motion of the end effector replicates a range of motion which is consistent with surgical procedures, and all constraints are kept intact throughout the entire simulation; thus, this design appears to be quite functional.

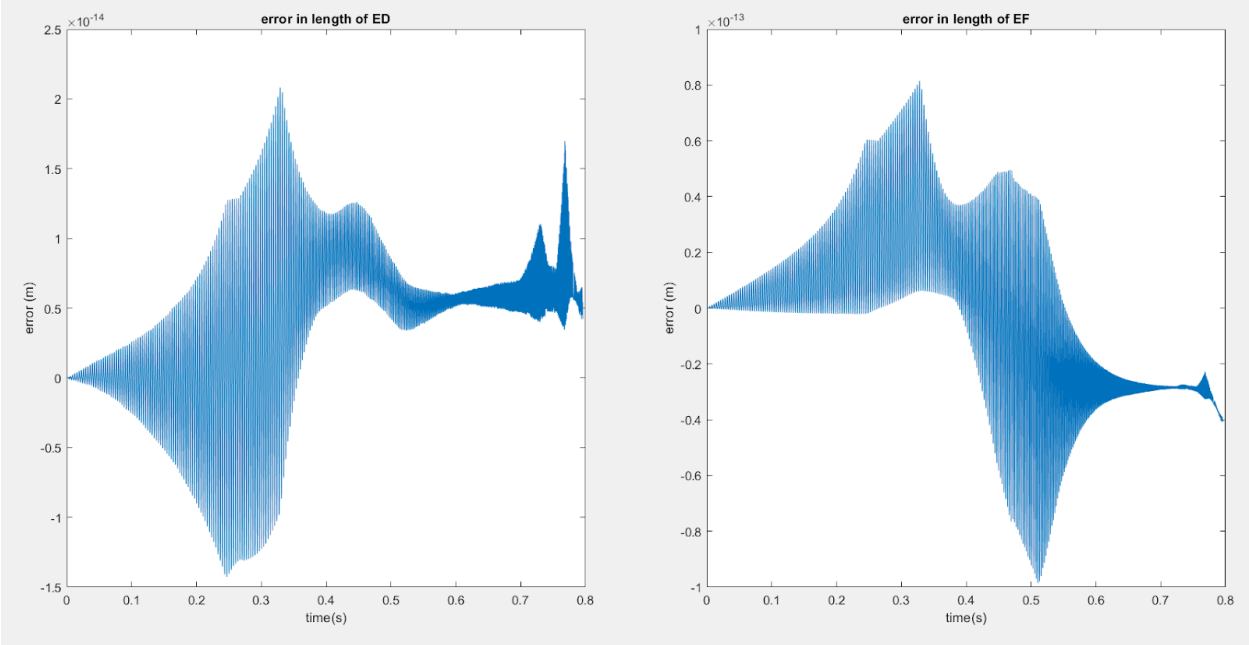

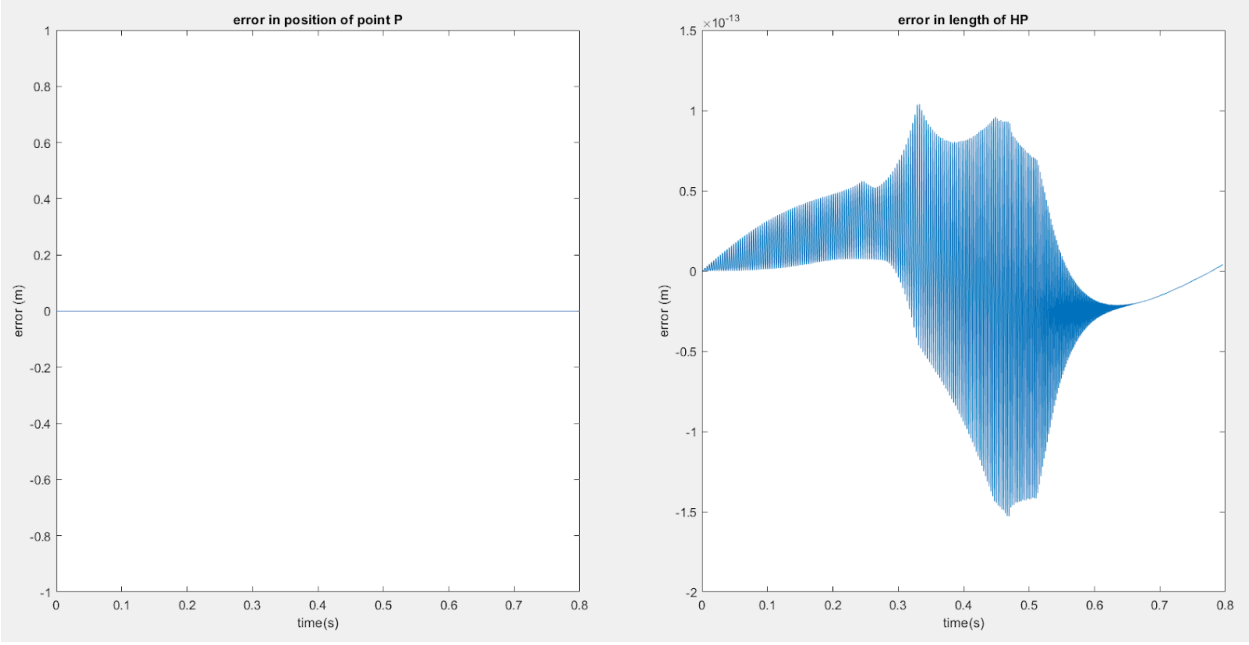
error in position of point P
error (m)
time(s)
error in length of HP
×10^-13
error (m)
time(s)

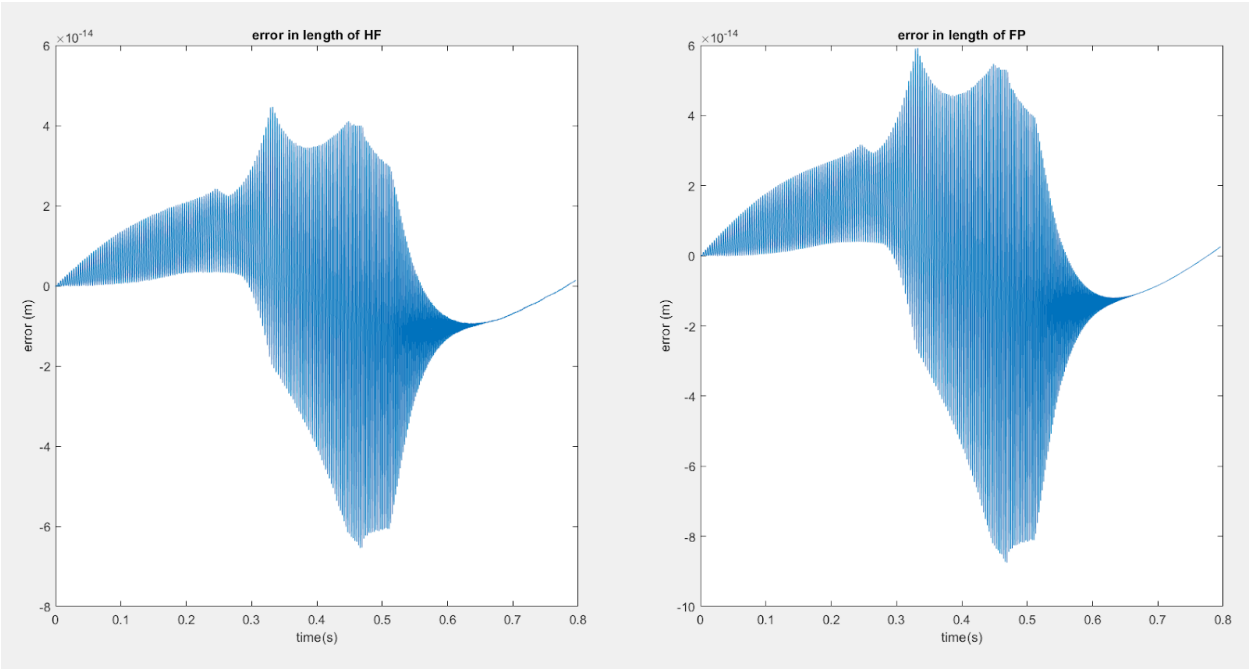
error in length of HF
×10^-14
error (m)
time(s)
error in length of FP
×10^-14
error (m)
time(s)